MATHEMATICAL BIOSCIENCES
AND ENGINEERING
Volume **12**, Number **4**, August **2015**

doi:10.3934/mbe.2015.12.879

pp. **879–905**

MATHEMATICALLY MODELING THE BIOLOGICAL PROPERTIES OF GLIOMAS: A REVIEW

Nikolay L. Martirosyan[1], Erica M. Rutter[2], Wyatt L. Ramey[3]

Eric J. Kostelich[2], Yang Kuang[2] and Mark C. Preul[4]

[1]Division of Neurosurgery, University of Arizona
Tucson, AZ 85724, USA
[2]School of Mathematical & Statistical Sciences
Arizona State University, Tempe, AZ 85287, USA
[3]Creighton Medical School, Phoenix Campus
St. Joseph's Hospital and Medical Center, Phoenix, AZ 85013, USA
[4]Division of Neurological Surgery, Barrow Neurological Institute
St. Joseph's Hospital and Medical Center, Phoenix, AZ 85013, USA

Abstract. Although mathematical modeling is a mainstay for industrial and many scientific studies, such approaches have found little application in neurosurgery. However, the fusion of biological studies and applied mathematics is rapidly changing this environment, especially for cancer research. This review focuses on the exciting potential for mathematical models to provide new avenues for studying the growth of gliomas to practical use. *In vitro* studies are often used to simulate the effects of specific model parameters that would be difficult in a larger-scale model. With regard to glioma invasive properties, metabolic and vascular attributes can be modeled to gain insight into the infiltrative mechanisms that are attributable to the tumor's aggressive behavior. Morphologically, gliomas show different characteristics that may allow their growth stage and invasive properties to be predicted, and models continue to offer insight about how these attributes are manifested visually. Recent studies have attempted to predict the efficacy of certain treatment modalities and exactly how they should be administered relative to each other. Imaging is also a crucial component in simulating clinically relevant tumors and their influence on the surrounding anatomical structures in the brain.

1. **Mathematical models in medicine.** Over the last several decades, much research has been devoted to understanding the physical and biological properties of gliomas in the effort to develop an extensive knowledge of this disease. Mathematical models are vital to many disciplines of science. Yet, compared to other scientific disciplines, there has been relatively little effort within neurosurgery or neuro-oncology to exploit such knowledge to form predictive systems that could accurately model or simulate the behavior of a malignant glioma. Such modeling could improve our sense of growth and invasive patterns and might translate into a useful clinical tool.

2010 *Mathematics Subject Classification.* Primary: 58F15, 58F17; Secondary: 53C35.

Key words and phrases. Biomathematical modeling, forecasting, glioma, tumor growth simulation, invasion, proliferation.

The first two authors have contributed equally to this work. Corresponding author: kuang@asu.edu.

This review presents an up-to-date survey of several types of mathematical models to characterize, quantify, and predict the complex behavior of gliomas. Although there have been other review papers published on the mathematical status of glioblastoma modeling [21], numerous recent advances in the field necessitate a current review. We emphasize dynamical models of tumor growth, i.e., systems of ordinary and partial differential equations, in contrast to statistical models that seek to infer correlations between clinical measurements and patient outcomes. Although statistical methods can provide useful rules of thumb for estimating outcomes like patient survival or response to treatment, they provide little insight into glioma biology.

Cancer is an inherently multi-scale process and different types of models adequately describe different aspects of the proliferation and spread of gliomas. All of the time and spatial scales of glioblastoma are important, from individual cell interactions to the role nutrients and brain geometry play on the tumor. This paper includes both microscopic and macroscopic models to ensure that all aspects of glioblastoma growth are covered.

We discuss several types of models in this paper, all of which are useful for describing different aspects of glioblastoma evolution and growth: spheroid models, vascular models, morphological models, and treatment models. We begin this paper by introducing *in vitro* spheroid models in section 2, which serve as a basis for understanding the basic dynamics of the proliferation and diffusion of glioblastoma cells. They approximate the growth of glioblastoma when the tumor is small and includes many reaction-diffusion models. These models can be effective in simulating the initial growth of the tumor cells. Since these models are *in vitro*, there is ample opportunity to compare models with experimental data, which allows parameters related to basic tumor dynamics to be estimated. Section 3 explores current research related to vascular and metabolic models. As the glioma tumor grows in size, it requires more nutrients and begins to co-opt and create nearby vasculature to provide the necessary nutrition. How the tumors are affected by nutrition, angiogenesis, and tumor vasculature is of great interest since this has been shown to influence the invasiveness and aggressiveness of the tumor. Section 4 summarizes research regarding morphological models. Morphological models are imperative to understanding the characteristics of the glioblastoma and how those characteristics determine and affect the evolution of the tumor. The biological processes involved in tumor growth and spread, such as chemotaxis, haptotaxis, cell-cell adhesion are studied individually and combined, to determine their influence on tumor shape and growth rate. In section 5, the models covered relate to the efficacy of treatments and therapies in eliminating tumor growth and prolonging patient life. Once the tumor reaches a detectable size, some type of treatment such as resection, chemotherapy, or radiotherapy is applied. The treatment models are concerned with using one or more of these treatments in combination to advance therapeutic options for glioblastoma patients.

We conclude the paper in section 6 with a discussion on the use of imaging in current glioma models. to validate the mathematical models, it is helpful to have experimental or clinical data. Experimental data often arises from *in vitro* experiments, and are meant to help isolate parameter values which can be used for more complicated *in vivo* models. These experimental images are often coupled with the *in vitro* spheroid tumors described above. Clinical data includes MR images and CT scans to visualize actual gliomas. Oftentimes, these images may

be time series, which allows the researcher to observe how the tumor evolves as time passes. The mathematical models comparing with clinical images often feature finite-element models as well as models which incorporate the brain structure and shape. Qualitative comparisons of the simulated tumor and actual tumor can validate the predictive ability of the model. Quantitative comparisons appear to be much more difficult, as small uncertainties in the initial simulated tumor may drastically change the output at the end time series.

2. ***In vitro* multicellular tumor spheroid growth models.** *In vitro* experiments allow the investigator to model growth and other desired tumor properties without external influences, such as host-tumor and vascular interactions, unless specifically incorporated. Multicellular tumor spheroids, composed of an initially small number of cells, provide a closed system in which the regulation of prevascular tumor expansion via three-dimensional intratumoral interactions can be closely examined. Idealized experiments also allow investigators to develop and parameterize simple mathematical models of cell growth, the parameters of which can be used for more involved future models. The mathematical models covered in this section mainly include reaction-diffusion models, continuum models, and simple discrete models.

Chignola et al. [6] used a stochastic Gompertzian-like mathematical model to describe a positive correlation between tumor variability and asymptotic volume. The implications of this relationship suggest that the maximum size of a tumor can potentially be determined from the multiple growth kinetics identified in a single tumor. The development of a maximum volume signifies that any further expansion of the tumor spheroid results in a greater increase in volume than surface area, leading to a decrease in nutritive supply and central necrosis, because the spheroid lacks any sort of neovascularization [8, 11]. With this in mind, Deisboeck et al. [8] used their tumor spheroid model to illustrate that, at this critical volume, individual cell invasion was a means of increasing surface area, thus signifying a relationship between tumor size and the onset of invasion. In their *in vitro* assay, tumor spheroids were grown in an extracellular matrix (ECM) gel and their infiltrative properties analyzed. According to their model, not only does tumor volume, or proliferation, seem to influence invasion, but invasion can also stimulate proliferation. In the early stages of their model, tumor spheroid invasion rapidly occurs at 24 h followed by volumetric growth at 48 h and another round of invasion at 72 h, implying that invasion can indeed lead to proliferation. Furthermore, once cells have begun infiltration, it is proposed that they undergo intra-branch homotype attraction. According to this concept, migratory cells follow each other along a pre-formed path in response to autocrine and paracrine signals ultimately toward some nutrient source, which is indicative of a complex self-organizing adaptive bio-system [8].

Cellular automata are a class of discrete mathematical models that can produce realistic simulations of the behavior of individual cells. Cellular automata define "rules" by which the state of a given cell at the next time step depends on the state of some number of its nearest neighbors at the current time. Even simple nearest-neighbor rules can result in complex behavior; adjusting even a single parameter in the rules can reproduce, at least qualitatively, many of the complex interactions seen *in vivo* [28]. One such interaction that has profound effects on the invasion of glioma cells is cell adhesion.

In a two-dimensional simulation, Aubert et al. [3] inserted a probability threshold that quantified the strength of cell-cell adhesion to their cellular automaton (see

figure 1). The model is set up to have each cell be hexagonal, which is either free or occupied by a single cell. At each update, a cell may move only to the free hexagons surrounding it, but will remain where it currently is if the chosen updated position is already occupied. To account for cell-cell adhesion, a threshold value, $p \in [0, 1]$, is chosen. At each evolution, a random number $r \in [0, 1]$ is chosen, and if $r < p$ the cell moves to a position whose nearest neighbors are occupied, and opposite if $r > p$. As the adhesion parameter, p, varied from weak ($p = 0$) to strong ($p = 1$), the ability of individual glioma cells to invade surrounding normal tissue decreased. Simulations with $p = 1$ correlated best with experimental data, suggesting that cell adhesion plays an important role in the behavior of gliomas [3].

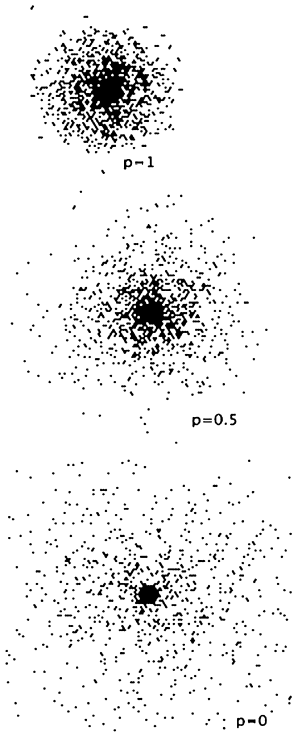

FIGURE 1. Simulated patterns of migration using different values of the probability threshold, which quantifies cell-cell adhesion. p=0 corresponds to a weak cell-cell adhesion, and p=1 corresponds to a strong cell-cell adhesion. (Source: Aubert M, Badoual M, Féreol S, Christov C, Grammaticos B. A cellular automaton model for the migration of glioma cells. Phys Biol. 2006 Apr 13;3(2):93-100. DOI:10.1088/1478-3975/3/2/001. Reproduced by permission of IOP Publishing.) [3].

Continuum mathematical models rely on differential equations to express growth dynamics in terms of rates of change of various quantities of interest. Unlike cellular automata, such models do not attempt to simulate individual cells; rather, they estimate population densities of cells at grid points within the computational domain.

As with cellular automata, model parameters related to cell adhesion strongly affect the cells' invasiveness, expressed in terms of rate of spread into regions of low cell density. Adhesion can affect the invasive properties of glioma cell lines that have historically been associated with increased aggression and malignancy. When a wild-type glioma (U87WT) was grown in a three-dimensional collagen gel *in vitro* assay, it exhibited greater invasiveness and a faster shed rate than the mutated cell line (U87ΔEGFR), which has an amplified expression of epidermal growth factor receptor (EGFR). Because the fit to experimental observations was optimal when higher parameters were used for undirected motility and shed rate for the wild type within the continuum model, these dramatic differences in phenotypes may be attributable to changes in cell adhesion. For example, cell-cell adhesion between ΔEGFR cells may increase. However, Stein et al. [53] proposed that the wild type cells have an increased affinity for collagen in the medium, indicating that they can more readily overcome cell-cell adhesions and infiltrate the surrounding matrix, thus exhibiting a greater degree of haptotaxis.

Stein et al. [53] also discovered that the proliferating cells and invasive cells need to be modeled separately as they exhibit drastically different behaviors. To further explain, we look to the equations governing the behavior of the cell core (proliferating cells) and the migratory cells. The tumor sphere radius is assumed to be increasing at a constant rate, v_c, and shedding invasive cells at a rate, s. The behavior of the invasive cells, $u_i(r,t)$ is as follows:

$$\frac{\partial u_i(r,t)}{\partial t} = \underbrace{D\nabla^2 u_i}_{\text{diffusion}} + \underbrace{g u_i\left(1-\frac{u_i}{u_{\max}}\right)}_{\text{logistic growth}} - \underbrace{v_i \nabla_r \cdot u_i}_{\text{cells leaving tumor}} + \underbrace{s\delta(r-R(t))}_{\text{shed cells from core}}$$

where $R(t) = R_0 + v_c t$, describes the radius of the proliferating cells at time t. R_0 is the radius of the tumor core at initial time, and v_c represents the velocity with which the tumor core radius increases. The parameters of the model are D, the constant diffusion rate, the intrinsic growth rate g, and the rate at which the migratory cells move away from the tumor core v_i. Their simulations showed that by separating the populations of proliferating cells and migratory cells, they were able to accurately model the behavior of migratory cells, when compared with experimental data (see figure 2) [53].

One limitation to reaction-diffusion type models is that uniform symmetric diffusion is assumed. For glioblastomas which have biased diffusions, higher-order models may be necessary. Fort and Sole [12] modeled beyond the standard reaction-diffusion-advection, and were able to show greater agreement with experimental data. They showed that cells do not move equally probable in all directions, but rather move in a bias towards the invasion front. Patient specific values, which can be measured for each patient, dictate the effect of biased dispersal, which can largely influence the tumor growth predictions and the efficacy of resection surgery [12].

The use of spheroids will continue to be a vital tool in the effort to predict tumor behavior. As with every method, however, there are limitations. *In vivo*, malignant gliomas are not regular spheroids; they are a heterogeneous composition of cells. When estimating the invasive radius of glioma cells, investigators usually draw a best-fit ring around the invasive area [64]. Stein et al. [54] proposed a novel algorithm, automated invasive radii estimation (AIRE), which predicts the invasive zone radius based on the graininess of a bright-field image (a function of cell density). At very high cell densities, such as in the tumor core, and at very low

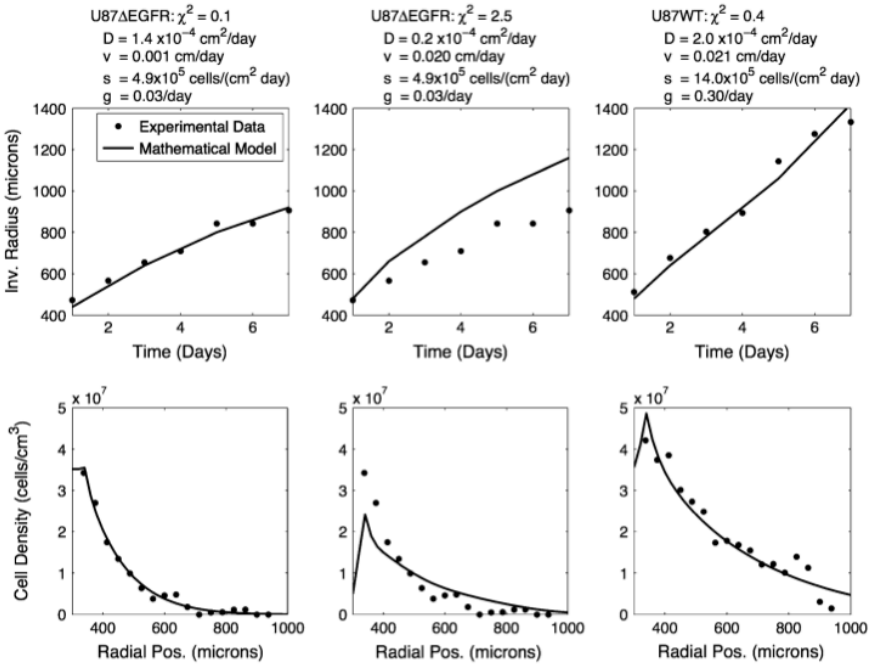

FIGURE 2. Simulations and experimental data plotted for U87WT and U87ΔEGFR with parameters listed. Both the invasive radius and cell counts are plotted. Note that the wild type U87 requires a much larger velocity bias to match experimental data. (Source: Stein, Andrew M., et al. "A mathematical model of glioblastoma tumor spheroid invasion in a three-dimensional in vitro experiment." Biophysical journal 92.1 (2007): 356-365. Used with permission from Cell Press.) [53].

cell densities, such as outside the invasive zone, graininess can be expected to be very low. However, at intermediate cell densities, such as in the infiltrative zone, graininess is expected to be high. The algorithm quantifies this value to provide an automated measurement of cell density and radius. Since many spheroid-based models use invasion area and cell density as a function of time, AIRE can provide investigators more accurate measurements in addition to decreasing calculation time and resources for future studies. Eventually, it may be possible to develop this algorithm to automatically calculate infiltrative radii in actual patient computed tomography (CT) and MR images [54].

3. **Metabolic and vascular models.** As noted with the growth of *in vitro* spheroids, glioma growth is thought to begin avascularly, followed by angiogenesis and vascular tumor growth [1]. A growing tumor requires a lot of nutrients, and once a tumor reaches a certain size, it begins to co-opt existing vasculature and to grow new vasculature to met those demands. The models in this section are concerned with not only the effects of glucose, oxygen, and other necessary nutrients, but also the growth and maintenance of the vasculature required to deliver them. In

this section, for modeling purposes, the tumor cell population often is divided into normal, hypoxic, and necrotic cell components, all of which function differently. The separation into different cell types has been show to allow researchers to model all types of dynamics visible in gliomas, as well as create conjectures on how the phenotypic switch from proliferative tumors to migratory tumors is achieved. The mathematical models discussed in this section include compartmentalized models and more involved cellular automaton models.

Tumor growth may progress by vessel co-option, blood vessel regression, and then growth, a process mediated by three key proteins: vascular endothelial growth factor (VEGF), angiopoietin-1 (Ang-1), and angiopoietin-2 (Ang-2) [17,24,25]. Models evaluating such conditions tend to focus on the microstructure of the tumor. Gevertz and Torquato [17] developed a cellular automaton that describes brain tumor growth along with the evolution of microvasculature. Their model confirmed that upregulation of Ang-2 in the presence of functional VEGF induced angiogenesis, whereas Ang-2 alone caused vessel regression. Potential treatment strategies that may prevent vascular growth and decrease tumor aggressiveness were discussed.

Since the VEGF-VEGFR complex forms in response to vessel regression and hypoxia, thereby stimulating angiogenesis, blockage of this pathway may prevent tumor growth to a macroscopic size and clinical relevance. Alternatively, one may predict the inhibition of Ang-2 will reduce tumor growth. However, while angiogenesis will not occur, neither will vessel regression, meaning the tumor can survive and grow from co-opted vessels as predicted by the model. According to these simulations, an effective treatment will inhibit angiogenesis and allow vessel regression, which would prevent tumor from growing beyond a diameter of 1–2 mm [17].

Tumor microvasculature is also known to play a key role in the efficiency of tumor cells' glycolytic phenotype and its function in invasion. The glycolytic phenotype is the exclusive use of anaerobic metabolism in tumor cells, causing them to produce relatively large quantities of acid, which may aid invasion. By using a modified cellular automaton and partial differential equations, Gatenby and Gawlinski [16] modeled the glycolytic phenotype in the early and late phases of tumor growth, respectively. Their simulations indicated that a critical point of normal tissue density, tumor tissue density, and excess acid concentration may confer a transformation from a benign to a malignant tumor. Microvessel density, within some optimal range, will promote this acid-mediated invasion. Below the ideal vessel density for a certain acid concentration, excessive H+ will be toxic even to the tumor cells, because the vasculature is unable to buffer sufficient amounts of acid. On the contrary, a vessel density above the optimal range buffers too much of the produced acid, thereby hindering the ability of tumor cells to invade the surrounding tissue [43]. This evidence offers potential routes of treatment to help further contain the tumor and decrease its invasion. One method would be to induce self-poisoning by increasing the amount of intra-tumoral acid through inhibiting angiogenesis or simply by increasing tumor acid production. Furthermore, increasing normal cells' tolerance to increased acid concentrations would enhance their ability to effectively wall off the tumor and decrease invasion [16]. In either case, the role of acid is clearly significant to tumor invasion and potential treatments.

The previously discussed models quantitatively analyzed particular effects of neovasculature. Frieboes et al. [13] used their functional collective cell-migration units (FCCMU) models, which are based on conservation laws, to distinctively depict the morphology of evolving neovasculature. Moreover, their simulations calculate tumor

cell spatial distribution and viability as a function of nutrient availability (figure 3). The result is a unique model that accurately predicts areas of viable cells, necrosis, and tortuous neovasculature, which is similar to *in vivo* observations.

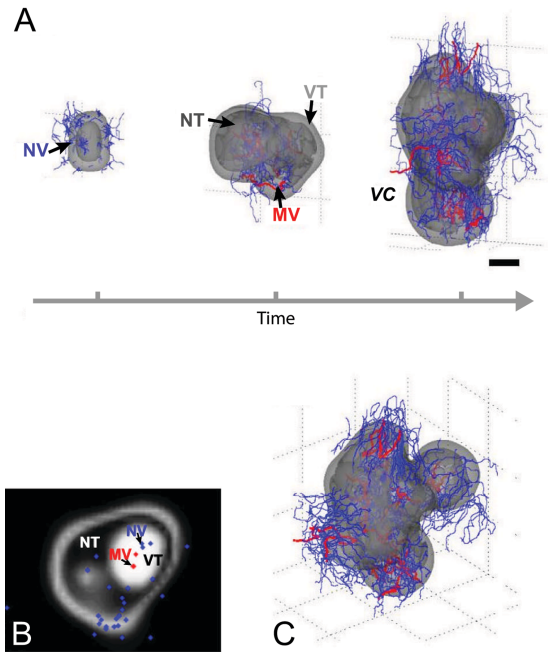

FIGURE 3. A multiscale three-dimensional computer simulation depicting a growing glioblastoma multiform (GBM). (A) A chronological simulation of growth over 3 months. VT and NT represent viable and necrotic tissue, respectively. MV and NV are mature blood-conducting vessels in red and new nonconducting vessels in blue, respectively. Neovascularization is shown here to affect morphology. (B) A histology-like section from the last frame seen in A. Areas of white represent viable tumor regions; darker regions within the section represent necrotic regions. (C) An additional view of the tumor depicted in the last frame in A. (Source: Frieboes HB, Lowengrub JS, Wise S, Zheng X, Macklin P, Bearer EL, Cristini V. Computer simulation of glioma growth and morphology. Neuroimage. 2007;37 Suppl 1:S59-70. Epub 2007 Mar 23. Used with permission from Elsevier.) [13].

As a glioma expands, its vasculature becomes less and less likely to provide oxygen and nutrients to all regions of the tumor. Consequently, areas of hypoxia are introduced to zones of lesser perfusion, resulting in more aggressive behavior. This hypothesis is supported by a positive correlation between relative hypoxia, the ratio of hypoxic tumor volume to a T2-defined tumor volume, and tumor aggressiveness, as quantified by the commonly used proliferation to diffusion rate ratio (ρ/D). Szeto

et al. [60] used preoperative 18F-fluoromisonidazole (FMISO)-positron-emission tolerance images and serial T1-weighted gadolinium and T2-weighted MR imaging to estimate patient-specific ρ and D values to predict tumor aggressiveness as a function of hypoxia.

Recent mathematical models have advocated treating these normoxic, hypoxic, and necrotic cells as separate populations. In 2011, Swanson et al. [59] created a compartmental model which separated normoxic, hypoxic, and necrotic glioma cells, in addition to vasculature and angiogenic factors. The authors showed that with this improvement, all dynamics of *in vivo* gliomas can be modeled. They propose that the interaction between tumor cells and their microenvironment are key to developing malignancy. Martinez-Gonzalez et al. [38] developed and studied a compartment style model which featured normoxic and hypoxic cells competing for resources. They discovered that when vaso-occlusive episodes cause hypoxic conditions, cell phenotypic switch occurs. They propose that attempting prevention of collapsing micro vessels in the tumor may slow glioma migration. Papadogiorgaki et al. [42] created a 3D multi-compartment continuum model which predicts avascular glioma growth in an isotropic and homogeneous medium. The model simulates both proliferation and migration by including interaction between four distinct glioma cell populations: proliferative, hypoxic, hypoglycemic and necrotic cells in addition to their tissue microenvironment. The effects of glucose and oxygen are taken into account both individually and combined. By compartmentalizing the model as described, the authors are able to see how subpopulations of the various types of cells proliferate and diffuse, specifically allowing the researchers to determine the evolution of the malignant tumor cells. This also leads to the ability to estimate tumor growth parameters, which are difficult to determine from experimental data [42].

Hatzikirou et al. [20] proposed that the actual transformation seen in glioma cells from a proliferative phenotype to an invasive one is not attributed to mutations only, but rather to hypoxia and their 'Go or Grow' mechanism. Evidence suggests that a mechanism for this manifestation could be the down-regulation of cadherins during hypoxia [56]. According to the authors of this model, direct support for their hypothesis can be found after glioma resection. When the tumor is removed, there are invasive cells that are not resected and experience a return to normoxic levels, facilitating their conversion back to the proliferative phenotype, thereby explaining the quick recurrence and proliferation after removal [20]. If only mutations were responsible for this switch to the proliferative phenotype, a much longer period between treatment and recurrence would be observed. An unrealistically high phenotypic change rate via mutations, 103 phenotypic changes/division, must be used in their model to achieve a recurrence in the length of time consistent with clinical observations. Simulations also indicate that when resources are scarce, a predominant invasive phenotype may produce a more fit tumor with a greater cell population than one with proliferative cells in the majority, further supporting the 'Go or Grow' postulate [20]. These findings signify that enhanced tumor oxygenation may be a means to decelerate tumor aggressiveness and metastasis, further demonstrating the importance of metabolism and neovasculature in the potential treatment of glioma.

4. **Morphology in glioma models.** Without doubt, morphology, both microscopically and macroscopically, is a decisive indicator of glioma growth and invasion. For this reason, an abundance of recent research has emphasized tumor morphology

and its prognostic indications. Several studies investigating different glioma characteristics and their effects on tumor morphology and evolution are reviewed in this section. Characteristics that are heavily studied include chemotaxis, haptotaxis, and cell-cell adhesion. Models in this section strive to capture the morphological phenomena observed *in vivo*, and furthermore, quantify the conditions necessary to create those phenomena. Models in this section are represented by more discrete models as well as reaction-diffusion models.

Glioma morphology can be studied in a straightforward manner with multicellular tumor sphenoids, which provide a relatively simple demonstration of growth characteristics. Two of the most fundamental foundations of glioma cell movement are chemotaxis and homotype attraction, which is the secretion of soluble paracrine-acting agents that attract similar cells [47]. In their discrete model of microscopic brain tumor growth characteristics using multicellular tumor sphenoids, Sander and Deisboeck [47] predicted invasive morphologies based on different strengths of chemotaxis and homotype attraction. Their simulations showed that a strong chemotaxis, either with or without a strong homotype attraction, was needed to induce invasion in a disc-like pattern around the tumor core. Turning off the chemotaxis and homotype attraction parameters produced a more compact area of randomly moving cells. Alternatively, when a very strong chemotaxis and very strong homotype attraction were implemented, the invasive zone was characterized by chain-like structures infiltrating the surrounding medium. This appearance was visually similar to migration of bacteria, but different biologically in the sense that bacteria tended to proliferate while in motion [47].

Haptotaxis, the movement of cells along some extracellular substrate like collagen or laminin, would make this model more complete. This parameter was closely examined in a discrete model investigating the relative influences of cell-ECM adhesion and cell-cell adhesion on invasion [63]. Cell-cell adhesion had less of an effect on depth of invasion than cell-ECM adhesion. However, reducing cell-cell adhesion in the presence of increased proteolytic enzyme secretion markedly increased invasion. This finding suggests that mutations decreasing cell-cell adhesion phenotypically emerge in the presence of substantially increased secretion of ECM-degrading enzymes, such as metalloproteinases (MMP), which aid in glioma invasion and growth [9, 63].

Turner and Sherratt [63] also studied the morphology of the infiltrating "advancing front." When forces of cell-ECM and cell-cell attraction equalized, a split occurred in the "fingers" of migratory cells. The split gave rise to a front of detached invasive cells governed by cell-ECM adhesion and a group of cells retreating to the main tumor mass governed by cell-cell adhesion. When a proliferation parameter was included in this simulation, fewer detached advancing fronts were observed. The "fingers" initially fixing the migratory cells to the main tumor mass were thicker and remained connected to the front longer because dividing cells were pushed forward, thereby oddly reducing invasion in this case. This comprehensive work suggests that therapies increasing cell-cell adhesion and reducing cell-ECM attraction may help contain glioma cells and prevent diffuse invasion [63].

Competition for nutrients and their availability through gradients also play a key role in glioma morphology. Through the use of a nutrient-limited, reaction-diffusion model, Ferreira et al. [10] showed that high nutrient consumption by normal cells

induced papillary, or finger-like, tumor morphologies due to decreased nutrient availability. Increased consumption of essential mitotic nutrients by cancerous cells also provoked more diffuse growth patterns (figure 4).

Ferreira et. al's model is similar to the previously mentioned Aubert et. al model, in that each individual cell is modeled in a structure. In this case, the tissue is modeled as a square lattice, and the capillary vessels, through which the nutrients diffuse, is located at the top of the lattice. There are there three types of cells in the tumor mass lattice: normal σ_n, cancerous σ_c, and necrotic cells σ_d. Only the cancerous cells can 'pile up' in one lattice cell. It is assumed that some nutrients are more important for the cancerous cells to grow and develop than others. The nutrients are separated into essential nutrients $N(\vec{x},t)$ and nonessential nutrients $M(\vec{x},t)$. The concentration fields of these nutrients is governed by the following non-dimensionalized equations:

$$\frac{\partial N}{\partial t} = \underbrace{\nabla^2 N}_{\text{diffusion}} - \underbrace{\alpha^2 N\sigma_n}_{\text{absorption into normal cells}} - \underbrace{\lambda_N \alpha^2 N\sigma_c}_{\text{absorption into cancer cells}}$$

$$\frac{\partial M}{\partial t} = \underbrace{\nabla^2 M}_{\text{diffusion}} - \underbrace{\alpha^2 M\sigma_n}_{\text{absorption into normal cells}} - \underbrace{\lambda_M \alpha^2 M\sigma_c}_{\text{absorption into cancer cells}}$$

where λ_N and λ_M represent the nutrient consumption rates of essential and nonessential nutrients by cancerous cells, and α represents the nutrient consumption rates for healthy cells.

Each individual cell in the lattice can be selected at random to perform cell division, cell migration, or cell death. In the case of division, if the cell is in the tumor, then the daughter cell occupies the same lattice square. If the cell is on the tumor border, then the daughter cell randomly occupies one of the nearest neighbor sites. The ability to divide is governed by the concentration of essential nutrients per cancer cell. The cancer cells can migrate with a certain probability. A cancer cell in the interior of the tumor moves to a randomly selected nearest neighbor site. The movement of cancer cells on the border depends on the number of cancer cells at each site. If there is only one cancer cell at a given border site, then it migrates by interchanging places with a neighboring "invaded" cell. Otherwise, migrating cells move to the position of the nearest normal or necrotic cell. The probability of migration is dependent upon the nonessential nutrients. Cancer cells die with a certain probability which is governed by the nonessential nutrients present on the selected cell. The probabilities for each of these actions are given below:

$$P_{\text{div}}(\vec{x}) = 1 - \exp\left[-\left(\frac{N}{\sigma_c \theta_{\text{div}}}\right)^2\right]$$

$$P_{\text{mov}}(\vec{x}) = 1 - \exp\left[-\sigma_c\left(\frac{M}{\theta_{\text{mov}}}\right)^2\right]$$

$$P_{\text{del}}(\vec{x}) = \exp\left[-\left(\frac{M}{\sigma_c \theta_{\text{del}}}\right)^2\right]$$

Nutrient consumption by normal cells and essential nutrient consumption by cancer cells governed by the model parameters α and λ_N, respectively, were key in predicting tumor morphology and glioma shape instability.

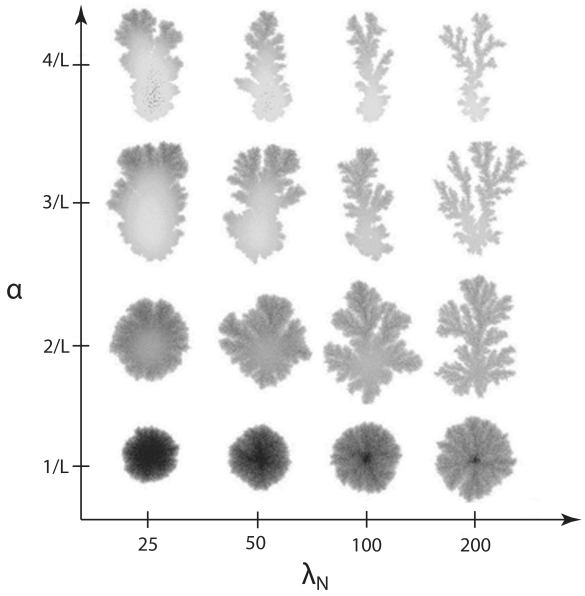

FIGURE 4. Along the y-axis, α represents the nutrient consumption for normal cells and increases moving up the axis. Along the x-axis, λ_N represents the consumption rate of mitotic essential nutrients by the cancer cells and increases moving along the axis. Darker regions are indicative of high cancer cell densities. For low normal cell and tumor cell nutrient consumption, an abundance of nutrients is available, which is why the tumor can thrive with a compact morphology. As normal cell and tumor cell nutrient consumption increases, a shortage of nutrients develops as the morphology becomes more papillary. (Reprinted figure with permission from: Ferreira SC Jr, Martins ML, Vilela MJ. Reaction-diffusion model for the growth of avascular tumor. Phys Rev E Stat Nonlin Soft Matter Phys. 2002 Feb;65(2 Pt 1):021907. Epub 2002 Jan 23. DOI: 10.1103/PhysRevE.65.021907. Copyright 2002 by the American Physical Society.) [10].

Frieboes et al. [14] also investigated the nutrients' outcome on morphology and through their reaction-diffusion model provided further support that nutrient gradients potentially have a direct impact on tumor morphology and invasion. To reinforce their findings, the authors demonstrated that formation of sub-tumors, which are a group of cells growing away from the main tumor mass, was the result of nutrient diffusion gradients and not hyper-proliferation of a single cell. Half the cells in a spheroid were stained one color and the other half were stained another color. The spheroid was allowed to grow within the experimental parameters. The resulting sub-tumors were comprised of cells of both colors, indicating one hyper-proliferative cell was most likely not responsible for the sub-tumor outcroppings.

Kim and Roh [30] reported that the inclusion of cell-cell adhesion, in addition to random diffusion, chemotaxis, and haptotaxis, led to the ability to see all migration patterns that have been reported previously in experiments. The morphology of the migrating cells shifting from branching to dispersion depending on the values

of the adhesion, haptotactic, and chemotactic parameters. In further detail, the chemotactic sensitivity, which is related to the tendency of the cell to move into glucose-rich areas, controls the speed of migration. Additionally, as cell-cell adhesion is increased, the speed of the front of the migration decreases, which offers the possibility of therapy which would cause over expression of the cell adhesion molecules. Gao and Wei [15] perform a full analysis of the mathematical model to prove the existence of a unique global solution.

Godlewski et al. [18] determined that a single microRNA influenced proliferation, migration, and sensitivity to glucose deprivation. The microRNA, miR-451 regulates the balance between proliferation and migration: higher levels of glucose increase the levels of miR-451, which causes elevated cell proliferation, lower levels of glucose decrease the levels of miR-451, which in turn enables the glioma cells to migrate. Kim et al. [32] incorporated miR-451 into a mathematical model, which shows how the levels of glucose affect cell proliferation and migration. Their findings include that if the glucose levels fluctuate, tumor growth and spread is faster. They propose that drugs which upregulate miR-451 act to slow down the migration of the glioma cells, which could impact efficacy of resection.

To summarize the notion that tumor cell substrates affect morphological patterns seen in gliomas, Bearer et al. [4] proposed tumor growth and invasion are predictable and quantifiable processes guided by substrate gradients and regulated by genotypic, phenotypic, and microenvironmental parameters. They used a multiscale mathematical model of tumor evolution, which considered phenotype, genotype, and morphological parameters, to consistently and accurately simulate all known invasive microscopic morphologies, such as chains, detached clusters, and protruding "fingers" [4, 7, 13, 66, 69]. The authors suggested that these migrating cells enlarge their surface exposure to substrates by avoiding a compact globular morphology. Finally, this mathematical model predicted that the observed invasive morphologies were linked to genotypic and phenotypic changes dependent on substrate gradients and other microenvironmental parameters, thereby exhibiting the growth phase of the tumor and its clinical relevance [4].

5. **Modeling radiotherapy, chemotherapy, and glioma resection.** While most aspects of studies reviewed thus far have involved simulating the endogenous properties of gliomas, we now consider models that include the effects of implementing various forms of treatment in an attempt to determine their efficacy and to propose better therapeutic options. These models usually depict tumor changes on a larger scale, and often include full brain geometry. As mentioned, the length of survival after a glioma is diagnosed has improved little in the last several decades. Therefore, it is necessary to be able to model therapies and illustrate why they work or how they can be improved. The main therapies studied in this section include resection, or the removal of the main tumor mass, chemotherapy, and radiotherapy. These therapies are studied alone and in conjunction with one another in hopes of increasing patient survival time.

Relative to radiotherapy, recent work has accurately outlined therapeutic success with regard to resection and *in vivo* tumor responses during treatment. According to a four-dimensional computer modeling system that used a cubic mesh superimposed on a tumor and its anatomical surroundings, an increase in clonogenic cell density (CCD), the number of proliferating tumor cells, renders the tumor more difficult to treat, resulting in quicker regrowth after a short pause in radiation, such

as on weekends during a treatment regimen [52]. The highest CCD in the tumor is assumed to be in the proliferating layer, where it is twice that of the G0 layer and 10 times that of the necrotic layer. The authors also reported that an accelerated hyperfractionated (AHF) schedule allows the tumor to grow to the original total number of cells faster than the hyperfractionation (HF) schedule [52]. This finding suggests that for aggressive tumors HF may lengthen the time till full recurrence. That is, tumor cells eluding death at the end of AHF irradiation began to proliferate and considerably outnumbered cells that evaded irradiation at the time HF was terminated. Also of great importance to glioma response during radiotherapy was the degree of hypoxia in the tumor. The oxygen enhancement ratio (OER) quantified hypoxia and positively correlated with tumor radioresistance. Although these findings may seem to simulate the obvious, the authors point out that their model represents a way to further quantify the relationships seen in a dynamic and complex tumor environment [52].

Stamatakos et al. [51] used a similar model but simulated chemotherapy with the drug temozolimide (TMZ) in hopes of merging it with a study comparable to the study mentioned above. Two different fractionation schemes and how they affected treatment outcome were investigated. Based on these simulations, giving TMZ once a day for the first 5 days in a 28-day schedule was more effective at decreasing the total number of metabolically living tumor cells than giving the same 5 doses uniformly throughout the 28-day schedule, a result that is consistent with clinical observations [51]. The same assumptions involving CCD in different tumor regions were used here as in the previous study, an improvement to previous work that used only two subpopulations of tumor cells, those susceptible and those resistant to chemotherapy [62]. Radiotherapy with concurrent chemotherapy increases survival times, and a reaction-diffusion mathematical model has shown that concurrent chemotherapy can increase median survival time by 2.5 months [55].

Another method that has been used to measure the efficacy of radiotherapy is the comparison of an untreated virtual control (UVC) to actual patient data. Within the UVC, survival time of the untreated scenario is estimated using a fatal tumor burden, which is measured in one of two ways: a fatal tumor radius or a fatal number of tumor cells. Swanson et al. [58] used patient-specific parameters of ρ, D, and v (proliferation, diffusion, and the radial expansion velocity of the glioma), obtained from two serial MRIs of patients before treatment to simulate the UVC and to estimate an untreated survival time based on the fatal tumor burden. This projected life expectancy was compared to the actual survival time of the treated patient and showed at least qualitatively some degree of radio-sensitivity or radio-resistance. Also of interest is not only the untreated virtual control, but also estimating the time when the tumor began growing as a means of trying to understand what can cause glioblastoma. Murray has used methods to estimate both the time from tumor initiation to tumor detection as well as the time from tumor detection to death from tumor burden [41]. Wang et al. [65] follow a very similar approach in quantifying the therapeutic response index. This index is a ratio of the actual survival time to that of the UVC, thus indicating the effectiveness of treatment for a patient. A positive correlation was observed between therapeutic response index and net proliferation.

Since it has been observed that radio-sensitivity exists, studies have attempted to quantify and estimate a value for the overall radio-sensitivity of a tumor. Rockne et al. [46] assumed a typical response window of -30% to +20% change in pretreatment

radius immediately after cessation of treatment. This assumption was based on data from the RECIST (Response Evaluation Criteria in Solid Tumors) criteria. Knowing the typical response window of gliomas to radiotherapy, the authors estimated a broad range in which the radio-sensitivity may lie. This value was applied to all cells of the tumor and an in silico simulation of response to radiotherapy was run. A larger value of radio-sensitivity indicated a higher net proliferation rate and greater tumor response. The obvious shortcoming of this model is that it used a broad range of radio-sensitivity for its simulations.

Further work has individualized this parameter based on the strong correlation with the net proliferation rate of a tumor. For each patient, multiple values of radio-sensitivity parameter were chosen and radiotherapy was simulated for each. The simulated and actual post-therapy T1-weighted gadolinium and T2-weighted MR images were compared, and a value of radio-sensitivity was calculated, through regression, to minimize the radii between the two images. Although future work should not discount the importance of undetectable infiltrative cells, there was no correlation between radio-sensitivity and the invasion rate. This finding suggests the degree of invasiveness may have no bearing on glioma response to radiotherapy [40]. To the authors' knowledge, this is the first instance of estimating a radio-resistance parameter for individual patients *in vivo*. It is more personalized than estimating cellular survival fraction from a standard dose of 2 Gy, as used by Kirkby et al. [33] and it is also more specific than using parameters from the broad RECIST criteria.

Due to the diffuse nature of gliomas, in particular GBM, surgical resection is typically viewed as a means to increase patient survival time rather than provide a cure. In a simplified model of glioma recurrence after resection, Alvord [2] explained that a tumor the size of the original mass can be observed in as few as 6 or 7 doubling times. As mentioned, it has been proposed that the usually non-proliferating infiltrative cells experience a return to normoxic levels upon resection, inducing a return to proliferative growth [20]. However, the time it takes for a GBM to regrow to its original size can be extended with subsequent radiotherapy and chemotherapy. One area under investigation with respect to this is the manner in which to administer these two treatments. Using a reaction-diffusion model, Powathil et al. [44] demonstrated that postoperative radiotherapy was more effective when given with neo-adjuvant, concurrent, and adjuvant chemotherapy compared to only concurrent and adjuvant chemotherapy. Based on their model, the authors proposed that concurrent chemotherapy affects only invasive cells; the neo-adjuvant method, however, affects all tumor cells temporally while radiotherapy kills remaining cells in the target area.

Tian et al. [61] conducted another experiment that models the efficacy of postoperative radiation and chemotherapy and further included the radius of resection as a means to quantify the degree of removal. The model is radially symmetric tumor, with a radius at resection time of $R_0 = 20$ mm. After partial resection, a smaller sphere of radius R_* is removed, and is filled with cerebrospinal fluid. The model describes the behavior of the remaining shell of the tumor as it undergoes radiotherapy and chemotherapy. The total number of cells is constant, with x as the tumor stem cell density and y as the dead cell density. $r = R(t)$ denotes the boundary of the tumor, which determines the survival of the patient - tumors which

reach 40 mm are assumed to be fatal. The governing equations are as follows:

$$\frac{\partial x(r,t)}{\partial t} + \frac{1}{r^2}\frac{\partial}{\partial r}(r^2 u(r,t)x(r,t)) = \underbrace{\lambda x(r,t)}_{\text{proliferation}} - \underbrace{\delta x(r,t)}_{\text{lysis}} - \underbrace{A\rho(t)x(r,t)}_{\text{radiotherapy}} - \underbrace{B\tau(t)x(r,t)}_{\text{chemotherapy}}$$

$$\frac{\partial y(r,t)}{\partial t} + \frac{1}{r^2}\frac{\partial}{\partial r}(r^2 u(r,t)x(r,t)) = \underbrace{\delta x(r,t)}_{\text{lysis}} + \underbrace{A\rho(t)x(r,t)}_{\text{radiotherapy}} + \underbrace{B\tau(t)x(r,t)}_{\text{chemotherapy}} - \underbrace{\mu y(r,t)}_{\text{dead cells}}$$

$$\frac{\theta}{r^2}\left(\frac{\partial}{\partial r} r^2 u\right) = (\lambda + \mu)x(r,t) - \mu\theta$$

$$\frac{dR}{dt} = u(R(t),t)$$

where $u(r,t)$ denotes the radial velocity of the tumor at time t and radius r. λ represents the proliferation rate of the tumor cells, δ the lysis rate of the tumor cells, and μ the removal rate of the necrotic cells. The radiation parameters include A, the rate at which radiation kills cells, and B the Temozolomide killing rate.

This mathematical model showed that for a tumor with an original radius 20 mm, resection followed by radiotherapy yielded a survival time of 52 weeks and 46 weeks when the radii of resection were 19 mm and 18 mm, respectively. This study thus quantified the common view that greater removal lengthens survival. Interestingly, postoperative radiotherapy distributed over 12 weeks instead of the standard 6 weeks increased survival time by about 4 weeks. However, when the standard dose of 60 Gy was doubled, survival increased from 46 to 80 weeks. However this model failed to include the toxic effects that excessive radiation would have on normal cells, a parameter that could be included in future improvements of the model [61]. Analysis of the mathematical model is presented in great detail by Yang et al. [67] which finds necessary conditions for the combination of radiation and chemotherapy to ensure tumor eradication.

Similarly, a comprehensive study by Eikenberry et al. [9] used a continuous reaction-diffusion model based on actual patient MR imaging data. Their model was capable of demonstrating the effects of surgical resection, radiotherapy, and chemotherapy to show both quantitatively and qualitatively that resection is more beneficial when followed by radiotherapy. Moreover, the model showed that the origin of the glioblastoma affected diffusiveness and invasion, thus affecting surgical outcome. Tumors originating deep within the brain, particularly around the ventricles, were more aggressive and had greater mass than those of superficial origin, while tumors from the brain stem and temporal lobes were shown to be larger than superficial but smaller than deep. This evidence has correlated with metabolic imaging studies of human gliomas *in vivo* [48]. Finally, to apply their model to an actual clinical scenario, the authors simulated the 20-month history of GBM, which is notable for resection at diagnosis, 8 months, and 14 months, and standard radiation and Gamma Knife treatment as well as chemotherapy after the initial resection. The model incorporated three- and two-dimensional simulations. However the three-dimensional modeling required the computational power of a supercomputer, whereas a two-dimensional model was far less intensive computationally and entailed fewer parameters. Their model results showed a course of progression qualitatively comparable to the actual MR images of the patient. Their findings verified

that their approach has the potential to depict behaviors of invasion and the outcomes of different treatments realistically [9]. However, their findings will need to be verified with additional subjects and scenarios.

Kim [29] proposed a larger-scale hybrid model in hopes of determining therapeutic approaches to eliminating the invasive glioma cells after resection has occurred, which includes exploiting their earlier discoveries about the effect of glucose and miR-451 on tumor migration and proliferation [32]. The simulated therapy would include injecting chemoattractants at the resection site to attract migratory tumor cells back to the original tumor area. This would be closely followed by glucose injections, which would lead to higher levels of miR-451, inducing cell proliferation, and more importantly, stifling cell migration. A follow-up surgery would then be used to eliminate the new tumor mass – ostensibly with no outlying invasive tumor mass [29, 31]. The authors do mention potential setbacks, however, including that if the glucose injection is initiated too early, it may induce proliferation in the dispersed tumor mass, leading to a worse outcome. Other potential setbacks include how to ensure that a high enough level of miR-451 to ensure there is no glioma cell migration, a concern which was recently addressed. As long as the administrations are spaced close enough together, the glioma cells will stay on the path to proliferation instead of migration [50].

6. **Use of imaging in glioma models.** Advances in MR imaging and CT technology have led to impressive improvements in the visualization of gliomas. Nevertheless, it remains difficult to correlate the imaging appearance of tumors like glioblastoma with the local density of viable cells. Although the location and extent of the tumor core can be identified with good accuracy, there are few data with which to quantify tumor cell populations in edematous and other more distant regions. In addition, although commonly held to represent the most active or dense areas of glioblastoma tissue, the high signal from MR contrast agents such as gadolinium do not necessarily equate to regions of increased tumor cell density. As well, areas of radio necrosis may not be distinguished from tumor using conventional MR imaging techniques, but require techniques such as MR spectroscopy, positron emission tomography, or other nuclear isotope scanning techniques [27, 45, 49]. Hence, MR images and CT scans cannot be used directly to estimate the initial conditions for continuum models of tumor growth. Future research efforts directed at this question would help computational scientists devise and parameterize continuum models that might make useful quantitative predictions, perhaps over periods of weeks to months, of the growth and spread of gliomas in individual cases. Models in this section often include full brain geometry to be able to compare with patient images, and also take into account white and gray matter, mass effect, and diffusion tensor imaging. Many of the models in this section are finite-element models.

With the use of the mechanical and anatomical properties of the brain, some mathematical models employ the finite-element method to model brain deformations in response to tumor growth and surgical intervention [19, 37]. Using their biomechanical model and an actual patient's image, Kyriacou et al. [37] deduced the appearance of the normal anatomy before disease via a biomechanical contraction or subtraction of the effects of a tumorous. This new "normal" image was compared to an atlas for a normal-to-normal atlas registration. After this step, a nonlinear regression scheme determined the tumor's origin and growth properties based on the previously seen anatomical deformation. This approach has interesting

potential for modeling mass effect and tissue displacement effect. However, it cannot calculate the effects of surrounding tissue stresses on the shape of the tumor, a parameter that is essential for depicting irregular surface growth of the visible tumor and mass effect [37]. Although it is convenient to use a standardized brain atlas as a template for simulations, there may be significant anatomical differences between the atlas and the patient.

Mass effect has been a perplexing problem for the development of tumor models that primarily use patient imaging data. Accurately modeling such anatomical deformations, often at a substantial distance from the tumor, is a critical step in being able to offer pre-treatment guidance. An inverse estimation method using complex partial differential equations was developed to drive a model that used the smallest possible number of patient-specific parameters to precisely and efficiently simulate growth and mass effect in a realistic clinical setting. With the comparison of 21 landmarks between actual and modeled images, a reasonable correlation was observed between the patient's target image and the model. Any uniformity of tumor growth in the simulation was a result of the brain being segmented into white matter and ventricles only. The results also indicated that the use of a small number of patient-specific and biologically driven parameters is sufficient to accurately model glioma behavior [23].

To account for large deformations, edema can be modeled spherically around the tumor as a soft material. Hogea et al. [22] used this method to quickly and efficiently measure mass effect, but the approach is sometimes inaccurate. To determine if the efficiency of similar models was heavily outweighed by the accuracy of slower, more complex and costly models, Zacharaki et al. [68] compared what they refer to as the nonlinear Lagrangian approach, a finite element formulation, and the piecewise linear Eulerian method, which employs a linear elastic, incremental pressure model [22, 40, 68]. The nonlinear Lagrangian method can be slightly more accurate with regard to comparative landmark errors, but its performance is about 10 times slower than the piecewise linear Eulerian method. The latter approach is likely to be the method of choice in an efficient and rapid image-based glioma model [68].

It is commonly assumed that glioma cells preferentially migrate faster in white matter than in gray matter, usually to a multiple of 5 [57]. Thus, not only is a heterogenic model of the brain pertinent for accurate simulation, but the anisotropic movement of glioma cells must be considered as well. Diffusion tensor imaging (DTI) is a means of three dimensionally viewing white matter tracts in a patient and can be used as a template to effectively demonstrate the anisotropic growth and invasion of a glioma. Within the same basic framework, anisotropic modeling more closely resembles *in vivo* tumor evolution than isotropic growth. It is sensitive to small changes in initial tumor location, indicating it could be an accurate a way to derive tumor origination [26]. However, although growth of the actual tumor is accurate, parameters to account for mass effect have not been included.

Bondiau et al. [5] proposed another model with a similar DTI component. However, they went further to include a biomechanical parameter for various cerebral anatomical structures, which allows proliferation of the tumor to depict mass effect. The basis of the mechanical model is to use linear elasticity to model the brain parenchyma behavior: relating stress to strain by $\sigma = k\epsilon$, with σ as the stress tensor, k the elasticity of the brain, and ϵ is linearized Lagrange stress tensor. In this case, k, varied depending on the structures of the brain: white matter, gray matter, skull, and falx all had differing values. The stress is modeled by $\epsilon = \frac{1}{2}(\nabla\chi + \nabla\chi^t)$,

where χ is the displacement of the point. From here, the governing mechanical equilibrium equation is written as follows:

$$0 = \underbrace{(\operatorname{div}\sigma)}_{\text{divergence of stress}} + \underbrace{F_e}_{\text{external forces on brain}}$$

Simulations agree well with patient MR images (figure 5). However, the DTIs were from a normal atlas. Consequently, the future use of DTI data from actual patients will be needed to personalize the model.

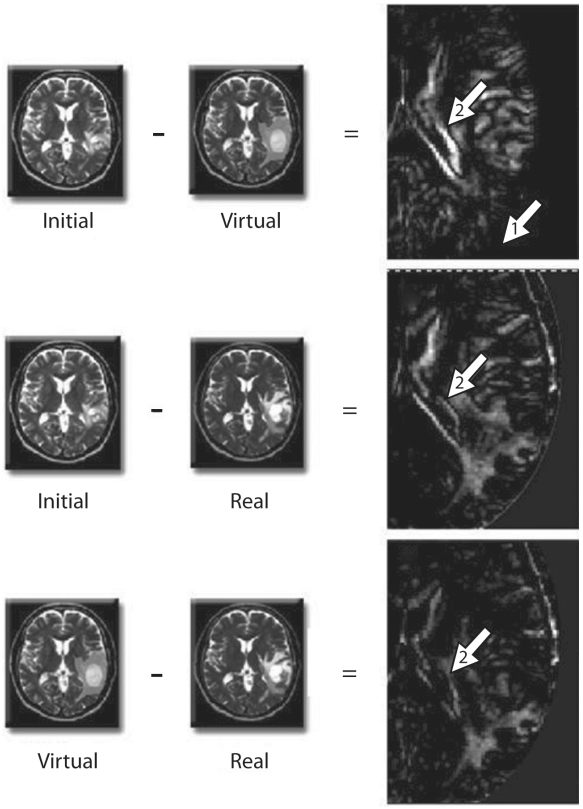

FIGURE 5. Correlations between various images used in the model. In the images along the right, areas of white depict large differences, whereas darker areas depict areas of similarity. (A) The image differences between the initial image and the final simulated virtual image, showing high variation in the ventricles (arrow 2). (B) Differences between the initial and final real patient image after 6 months, again showing areas of high variation in the ventricular area. (C) Differences between the simulated virtual and final real images. The dark gray next to the arrow indicates smaller variation in that area as opposed to the other comparisons. (Source: Bondiau PY, Clatz O, Sermesant M, Marcy PY, Delingette H, Frenay M, Ayache N. Biocomputing: numerical simulation of glioblastoma growth using diffusion tensor imaging. Phys Med Biol. 2008:879-93. DOI:10.1088/0031-9155/53/4/004. Reproduced by permission of IOP Publishing.) [5].

A recent attempt to personalize a model has come from applying a parameter estimation method to a reaction-diffusion model from serial MR images. Using the Eikonal approximation method with serial images, Konukoglu et al. [35] mathematically emulated the evolution of the tumor front (delineation) and, as a result, the speed of tumor growth in white and gray matter, thus characterizing brain inhomogeneities of that particular patient [34, 35]. The parameters can be estimated and applied to their reaction-diffusion model, simulating the tumor evolution. A fixed proliferation rate (ρ), regardless of the value, and the previously estimated patient-specific diffusion rates accurately depict tumor growth. This work represents a successful and exclusive simulation of tumor evolution and is supported by the strong correlation with actual patient images [35]. As mentioned, DTI of the actual patient would further personalize this model and make it more exclusive to the tumor under investigation.

Many of the previously cited models qualitatively compare images to their simulations to validate the model. Quantitative comparisons are much more difficult, however, since the final tumor shape is extremely sensitive to the initial condition of the tumor. To mitigate this issue, a mathematical procedure similar to that used in weather forecasting has been applied to simple models of glioma growth to assess, using synthetic data, the potential accuracy of forecasts of a glioma tumor in individual patients under reasonable assumptions regarding observational frequency and uncertainty and errors in model parameters. Because of uncertainties in initial conditions and the parameters of the model, the accuracy of a forecast often degrades with time. In the case of weather, predictions of a global numerical model are no more accurate than climatological averages after 10 to 14 days. Therefore, a method is needed to update the initial conditions based on recent observations and model forecasts. This process is called data assimilation. At operational meteorological centers, atmospheric measurements are combined with model forecasts to update the initial conditions of global models every 6 hours.

A proof-of-principle study by Kostelich et al. [36] showed that clinically useful forecasts of tumor growth for 60 days hence are potentially feasible. They assimilated synthetic magnetic resonance (MR) images from a control tumor into a set of forecasts at intervals of 60 days. That is, they ran a GBM growth model from statistically equivalent sets of initial conditions for 60 days to produce an ensemble of forecasts that are representative of the range of possible outcomes for a patient in two months' time. Next, the actual state of the patient (obtained from a new MR image) is used to update the forecasts to produce a new set of initial conditions. The model is run again for 60 days, and the process is repeated for a total of six cycles (360 days). Even in cases where there is a systematic mismatch between the model used to generate the control tumor and that used to generate the forecasts, there was still reasonable agreement between the control and the forecasts, provided that the data assimilation cycle was performed sufficiently often (60 days in this case). Figure 6 illustrates the results for the forecast and update cycle after 240, 300, and 360 days. The left column shows the "analysis mean" of the updated forecasts at each time point; red colors indicate higher tumor cell density. The middle column shows a color-coded representation, using the same color map, of the disagreement between the analysis mean and the control tumor (i.e., the "truth"). The right column shows the mean of the forecast ensembles, started from the same set of initial conditions (on day 1) as those in the left column, but without assimilating any intermediate synthetic MR images to update the model state vectors. This

study demonstrated that data assimilation methodologies used for weather prediction may be applicable to efforts to predict medical disease progression [39]. Such efforts, once they are validated, may one day be useful for patient counseling and treatment planning.

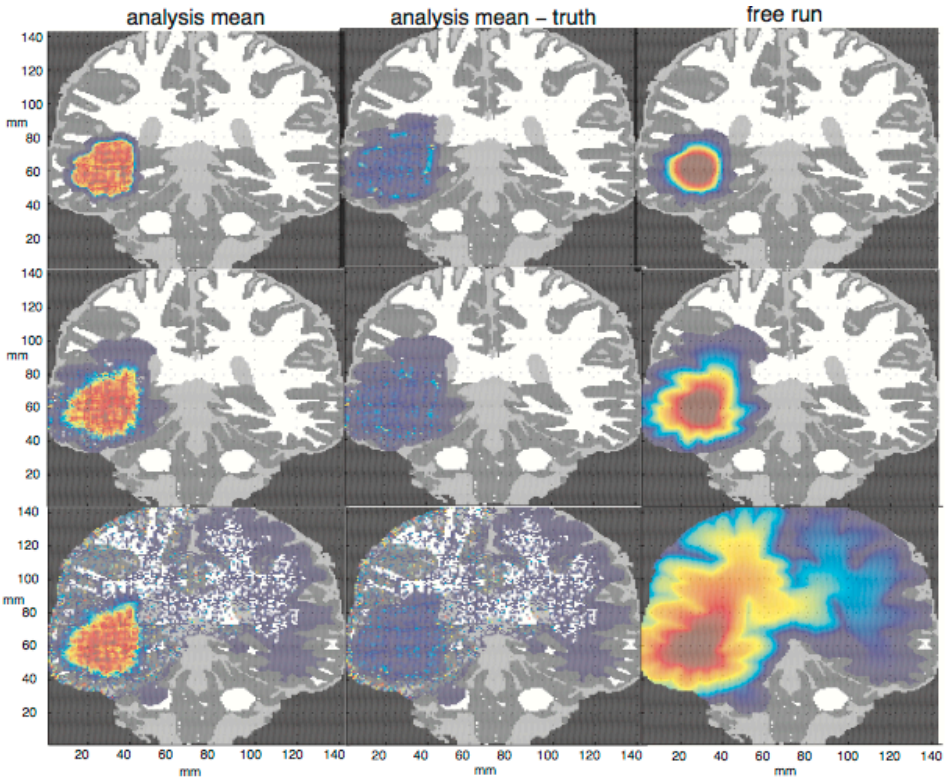

FIGURE 6. An image from Kostelich et al shows results of modeling a glioblastoma using Local Ensemble Transform Kalman Filter state estimation [36]. The first, second, and third rows show the results of forecasting from 240, 300, up to 360 days (top, middle, bottom rows, respectively). The left column shows the final ensemble analysis mean, and the middle column shows the pointwise absolute difference between the analysis mean and the "true" tumor. The right column shows the ensemble mean of free runs of the models, i.e., the mean 360-day forecast of tumor progression without the state update procedure. (Source: Kostelich EJ, Kuang Y, McDaniel JM, Moore NZ, Martirosyan NL, Preul MC. Accurate State Estimation from Uncertain Data and Models: An Application of Data Assimilation to Mathematical Models of Human Brain Tumors. Biol Direct. 2011; 6:64. Used with permission under the terms of the Creative Commons Attribution Liscense.) [36].

7. **Conclusion.** The mathematical models discussed in this paper range from radially symmetric 1D models to complicated 3D computational simulations. Each of the presented papers model a specific aspect of glioblastoma growth, morphology, or treatment. Spherically symmetric tumor models allow important parameters to

be accurately estimated, as they are also easy to replicate experimentally. Additionally, spherical models proved that there is drastically different behavior between the main tumor (proliferative cells) and migratory cells, which showed it is necessary to model tumor cells as separate populations, with differing behaviors [53]. As tumors reach a certain size, it becomes necessary to model the angiogenesis and growing vasculature. Several models have shown accuracy in predicting growth of vasculature as well as areas of normoxic, hypoxic, and necrotic cells within the tumor. Further models have included the effects due to haptotaxis, chemotaxis, and cell-cell adhesion and determined sensitivity of tumor growth due to these effects. Mathematicians have investigated the effects of not only biased diffusion, but also piecewise constant diffusion to accurately model how nutrients and tumor cells migrate through various brain tissue. The importance of glucose, oxygen and other nutrients has also been thoroughly investigated. In particular, glucose levels have been shown to directly influence tumor evolution - elevated levels of glucose increase cell proliferation and lower levels of glucose enables cell migration [32].

The previously mentioned models do show how the tumor and vasculature evolve throughout time, however, the effects of resection, radiotherapy, and chemotherapy are essential to clinical practice. Given the malignancy of glioblastomas, it is imperative that these tools are used intelligently to prolong the survival of the patient. Recently, mathematical and computational models have modeled mixtures of all three therapies, in an attempt to optimize patient survival times. Mathematicians have developed untreated virtual control (UVC) of patient data to compare the effects of radiotherapy without treating the tumor. This has led to development of a parameter estimation of the 'radiosensitivity' of a tumor - how well the tumor responds to radiotherapy. Others have shown experimentally that, contrary to what one would expect, the invasion rate of the glioma has no effect on response to radiotherapy. Some models incorporate resection in addition to radiotherapy and have determined radiotherapy administration schedules which might lengthen survival. The use of patient data to corroborate models is not common, but does exist in one model which qualitatively matched the effects of resection, radiotherapy, and chemotherapy [9].

The incorporation of experimental data, as well as imaging in the form of CT and MR is also discussed. These images act to further validate proposed mathematical models, although many of the comparisons remain qualitative in nature. These models act on a macroscopic scale, and delve into brain geometry and the influence this geometry has on the growth and migration of a tumor. As tumor growth is highly sensitive to parameters and initial conditions, a model has been proposed which 'corrects' itself when a new image is available.

Despite the progress that has been achieved so far, there are still many open biological questions to be addressed mathematically for glioblastomas. Although the effects of haptotaxis, chemotaxis, and cell-cell adhesion have been studied at length, there may be other mechanics that influence the spread and evolution of gliomas. How can the knowledge gained from these mathematical models further our biological understanding of the tumor evolution, and how might we exploit this understanding to mitigate the aggressiveness of a growing tumor? Other biological questions that remain unanswered include the role of genetic data in tumor progression. How does genetic data affect growth, and how can it be incorporated into

a relevant mathematical model? While the ultimate goal is to be able to use models to predict the growth and invasiveness of a tumor for a given patient, current models are not accurate enough to be used in a clinical setting yet.

Various mathematical models will become a vital tool in the understanding of gliomas. Similar to weather forecasting, the prediction of glioma behavior, as shown by the work in this article, is possible for short periods, beyond which new clinical data are required. Dynamic models, coupled with clinical measurements, may provide much more accurate predictions of glioma growth in individual patients than statistical models alone. As computational thresholds and interaction among scientists, clinicians, and mathematicians increase, the mathematical and biomechanical methods capable of modeling cancer biological behaviors are likely to become even more sophisticated. Such improvements may allow a precise system to be used in predicting the course of treatment after a glioma is diagnosed. As such modeling technologies become more sophisticated and reliable, they also may obviate the need for certain repetitious experiments involving the use of live scenarios. The numerous aspects of gliomas reviewed within these simulations are a means to develop models of such complexity. The ultimate goal is to forecast tumor growth individually for each patient, allowing growth pattern, velocity, and response to different treatment modalities to be estimated.

Until recently collaborations between neurosurgeons and mathematicians have been rare and focused on relatively esoteric topics. New research methods gained through interaction and collaboration with scientists outside mathematics, such as neurosurgeons, will encourage new approaches to what have been vexing clinical and research problems. Mathematical models will certainly be an intimate part of these new approaches toward the study and management of malignant gliomas. Such collaborations can be exciting, refreshing, and will likely generate better care for patients.

Acknowledgments. The authors thank the reviewer for his many helpful comments. Portions of this work were funded by the Barrow Neurological Institute Women's Foundation and by funds from the Newsome Family Endowed Chair of Neurosurgery Research held by Dr. Preul. E. R. and E. K. are partially supported by an ASU research grant. Y.K. was partially supported by NSF grant DMS-1148771.

REFERENCES

[1] T. Alarcón, H. M. Byrne and P. K. Maini, A multiple scale model for tumor growth, *Multiscale Modeling & Simulation*, **3** (2005), 440–475.

[2] E. C. Alvord Jr, Simple model of recurrent gliomas, *Journal of Neurosurgery*, **75** (1991), 337–338.

[3] M. Aubert, M. Badoual, S. Fereol, C. Christov and B. Grammaticos, A cellular automaton model for the migration of glioma cells, *Physical Biology*, **3** (2006), p93.

[4] E. L. Bearer, J. S. Lowengrub, H. B. Frieboes, Y.-L. Chuang, F. Jin, S. M. Wise, M. Ferrari, D. B. Agus and V. Cristini, Multiparameter computational modeling of tumor invasion, *Cancer Research*, **69** (2009), 4493–4501.

[5] P.-Y. Bondiau, O. Clatz, M. Sermesant, P.-Y. Marcy, H. Delingette, M. Frenay and N. Ayache, Biocomputing: Numerical simulation of glioblastoma growth using diffusion tensor imaging, *Physics in Medicine and Biology*, **53** (2008), p879.

[6] R. Chignola, A. Schenetti, G. Andrighetto, E. Chiesa, R. Foroni, S. Sartoris, G. Tridente and D. Liberati, Forecasting the growth of multicell tumour spheroids: Implications for the dynamic growth of solid tumours, *Cell Proliferation*, **33** (2000), 219–229.

[7] V. Cristini, X. Li, J. S. Lowengrub and S. M. Wise, Nonlinear simulations of solid tumor growth using a mixture model: Invasion and branching, *Journal of Mathematical Biology*, **58** (2009), 723–763.
[8] T. Deisboeck, M. Berens, A. Kansal, S. Torquato, A. Stemmer-Rachamimov and E. Chiocca, Pattern of self-organization in tumour systems: Complex growth dynamics in a novel brain tumour spheroid model, *Cell Proliferation*, **34** (2001), 115–134.
[9] S. E. Eikenberry, T. Sankar, M. Preul, E. Kostelich, C. Thalhauser and Y. Kuang, Virtual glioblastoma: Growth, migration and treatment in a three-dimensional mathematical model, *Cell Proliferation*, **42** (2009), 511–528.
[10] S. Ferreira Jr, M. Martins and M. Vilela, Reaction-diffusion model for the growth of avascular tumor, *Physical Review E*, **65** (2002), 021907, 8pp.
[11] J. Folkman and M. Hochberg, Self-regulation of growth in three dimensions, *The Journal of Experimental Medicine*, **138** (1973), 745–753.
[12] J. Fort and R. V. Sole, Accelerated tumor invasion under non-isotropic cell dispersal in glioblastomas, *New Journal of Physics*, **15** (2013), 055001, 10pp.
[13] H. B. Frieboes, J. S. Lowengrub, S. Wise, X. Zheng, P. Macklin, E. L. Bearer and V. Cristini, Computer simulation of glioma growth and morphology, *Neuroimage*, **37** (2007), S59–S70.
[14] H. B. Frieboes, X. Zheng, C.-H. Sun, B. Tromberg, R. Gatenby and V. Cristini, An integrated computational/experimental model of tumor invasion, *Cancer Research*, **66** (2006), 1597–1604.
[15] S. Gao and X. Wei, Analysis of a mathematical model of glioma cells outside the tumor spheroid core, *Applicable Analysis*, **92** (2013), 1379–1392.
[16] R. A. Gatenby and E. T. Gawlinski, The glycolytic phenotype in carcinogenesis and tumor invasion insights through mathematical models, *Cancer Research*, **63** (2003), 3847–3854.
[17] J. L. Gevertz and S. Torquato, Modeling the effects of vasculature evolution on early brain tumor growth, *Journal of Theoretical Biology*, **243** (2006), 517–531.
[18] J. Godlewski, M. O. Nowicki, A. Bronisz, G. Nuovo, J. Palatini, M. De Lay, J. Van Brocklyn, M. C. Ostrowski, E. A. Chiocca and S. E. Lawler, Microrna-451 regulates lkb1/ampk signaling and allows adaptation to metabolic stress in glioma cells, *Molecular Cell*, **37** (2010), 620–632.
[19] A. Hagemann, K. Rohr, H. S. Stiehl, U. Spetzger and J. M. Gilsbach, Biomechanical modeling of the human head for physically based, nonrigid image registration, *IEEE Transactions on Medical Imaging*, **18** (1999), 875–884.
[20] H. Hatzikirou, D. Basanta, M. Simon, K. Schaller and A. Deutsch, 'Go or grow': The key to the emergence of invasion in tumour progression?, *Mathematical Medicine and Biology*, **29** (2012), 49–65.
[21] H. Hatzikirou, A. Deutsch, C. Schaller, M. Simon and K. Swanson, Mathematical modelling of glioblastoma tumour development: A review, *Mathematical Models and Methods in Applied Sciences*, **15** (2005), 1779–1794.
[22] C. Hogea, G. Biros, F. Abraham and C. Davatzikos, A robust framework for soft tissue simulations with application to modeling brain tumor mass effect in 3D MR images, *Physics in Medicine and Biology*, **52** (2007), p6893.
[23] C. Hogea, C. Davatzikos and G. Biros, An image-driven parameter estimation problem for a reaction–diffusion glioma growth model with mass effects, *Journal of Mathematical Biology*, **56** (2008), 793–825.
[24] J. Holash, S. Wiegand and G. Yancopoulos, New model of tumor angiogenesis: Dynamic balance between vessel regression and growth mediated by angiopoietins and VEGF, *Oncogene*, **18** (1999), 5356–5362.
[25] J. Holash, P. Maisonpierre, D. Compton, P. Boland, C. Alexander, D. Zagzag, G. Yancopoulos and S. Wiegand, Vessel cooption, regression, and growth in tumors mediated by angiopoietins and VEGF, *Science*, **284** (1999), 1994–1998.
[26] S. Jbabdi, E. Mandonnet, H. Duffau, L. Capelle, K. R. Swanson, M. Pélégrini-Issac, R. Guillevin and H. Benali, Simulation of anisotropic growth of low-grade gliomas using diffusion tensor imaging, *Magnetic Resonance in Medicine*, **54** (2005), 616–624.
[27] B. Kanberoglu, N. Z. Moore, D. Frakes, L. J. Karam, J. P. Debbins and M. C. Preul, Neuronavigation using three-dimensional proton magnetic resonance spectroscopy data, *Stereotactic and functional neurosurgery*, **92** (2014), 306–314.
[28] A. Kansal, S. Torquato, G. Harsh IV, E. Chiocca and T. Deisboeck, Simulated brain tumor growth dynamics using a three-dimensional cellular automaton, *Journal of Theoretical Biology*, **203** (2000), 367–382.

[29] Y. Kim, Regulation of cell proliferation and migration in glioblastoma: New therapeutic approach, *Frontiers in Oncology*, **3** (2013), p53.
[30] Y. Kim, S. Lawler, M. O. Nowicki, E. A. Chiocca and A. Friedman, A mathematical model for pattern formation of glioma cells outside the tumor spheroid core, *Journal of Theoretical Biology*, **260** (2009), 359–371.
[31] Y. Kim and S. Roh, A hybrid model for cell proliferation and migration in glioblastoma, *Discrete & Continuous Dynamical Systems-Series B*, **18** (2013), 969–1015.
[32] Y. Kim, S. Roh, S. Lawler and A. Friedman, mir451 and ampk mutual antagonism in glioma cell migration and proliferation: A mathematical model, *PloS ONE*, **6** (2011), e28293.
[33] N. F. Kirkby, S. J. Jefferies, R. Jena and N. G. Burnet, A mathematical model of the treatment and survival of patients with high-grade brain tumours, *Journal of Theoretical Biology*, **245** (2007), 112–124.
[34] E. Konukoglu, O. Clatz, P.-Y. Bondiau, M. Sermesant, H. Delingette and N. Ayache, Towards an identification of tumor growth parameters from time series of images, in *Medical Image Computing and Computer-Assisted Intervention–MICCAI 2007*, Springer, **4791** (2007), 549–556.
[35] E. Konukoglu, O. Clatz, B. H. Menze, B. Stieltjes, M.-A. Weber, E. Mandonnet, H. Delingette and N. Ayache, Image guided personalization of reaction-diffusion type tumor growth models using modified anisotropic eikonal equations, *IEEE Transactions on Medical Imaging*, **29** (2010), 77–95.
[36] E. J. Kostelich, Y. Kuang, J. M. McDaniel, N. Z. Moore, N. L. Martirosyan and M. C. Preul, Accurate state estimation from uncertain data and models: An application of data assimilation to mathematical models of human brain tumors, *Biology Direct*, **6** (2011), p64.
[37] S. K. Kyriacou, C. Davatzikos, S. J. Zinreich and R. N. Bryan, Nonlinear elastic registration of brain images with tumor pathology using a biomechanical model [mri], *IEEE Transactions on Medical Imaging*, **18** (1999), 580–592.
[38] A. Martínez-González, G. F. Calvo, L. A. P. Romasanta and V. M. Pérez-García, Hypoxic cell waves around necrotic cores in glioblastoma: A biomathematical model and its therapeutic implications, *Bulletin of Mathematical Biology*, **74** (2012), 2875–2896.
[39] J. McDaniel, E. Kostelich, Y. Kuang, J. Nagy, M. C. Preul, N. Z. Moore and N. L. Matirosyan, Data assimilation in brain tumor models, in *Mathematical Models and Methods in Biomedicine*, eds Ledzewicz U., Schattler H., Friedman A., Kashdan E., Springer, Berlin, (2013), 233–262.
[40] A. Mohamed and C. Davatzikos, Finite element modeling of brain tumor mass-effect from 3d medical images, in *Medical Image Computing and Computer-Assisted Intervention–MICCAI 2005*, Springer, **3749** (2005), 400–408.
[41] J. Murray, Glioblastoma brain tumours: Estimating the time from brain tumour initiation and resolution of a patient survival anomaly after similar treatment protocols, *Journal of Biological Dynamics*, **6** (2012), 118–127.
[42] M. Papadogiorgaki, P. Koliou, X. Kotsiakis and M. E. Zervakis, Mathematical modelling of spatio-temporal glioma evolution, *Theoretical Biology and Medical Modelling*, **10** (2013), p47.
[43] A. A. Patel, E. T. Gawlinski, S. K. Lemieux and R. A. Gatenby, A cellular automaton model of early tumor growth and invasion: The effects of native tissue vascularity and increased anaerobic tumor metabolism, *Journal of Theoretical Biology*, **213** (2001), 315–331.
[44] G. Powathil, M. Kohandel, S. Sivaloganathan, A. Oza and M. Milosevic, Mathematical modeling of brain tumors: Effects of radiotherapy and chemotherapy, *Physics in Medicine and Biology*, **52** (2007), p3291.
[45] M. C. Preul, R. Leblanc, Z. Caramanos, R. Kasrai, S. Narayanan and D. L. Arnold, Magnetic resonance spectroscopy guided brain tumor resection: differentiation between recurrent glioma and radiation change in two diagnostically difficult cases., *The Canadian journal of neurological sciences. Le journal canadien des sciences neurologiques*, **25** (1998), 13–22.
[46] R. Rockne, E. Alvord Jr, J. Rockhill and K. Swanson, A mathematical model for brain tumor response to radiation therapy, *Journal of Mathematical Biology*, **58** (2009), 561–578.
[47] L. M. Sander and T. S. Deisboeck, Growth patterns of microscopic brain tumors, *Physical Review E*, **66** (2002), 051901.
[48] T. Sankar, Y. E. Kuznetsov, R. W. Ryan, Z. Caramanos, S. B. Antel, D. L. Arnold and M. C. Preul, The metabolic epicenter of supratentorial gliomas: A 1 h-mrsi study, *The Canadian Journal of Neurological Sciences*, **36** (2009), 696–706.

[49] T. Sankar, N. Z. Moore, J. Johnson, L. S. Ashby, A. C. Scheck, W. R. Shapiro, K. A. Smith, R. F. Spetzler and M. C. Preul, Magnetic resonance imaging volumetric assessment of the extent of contrast enhancement and resection in oligodendroglial tumors: Clinical article, *Journal of neurosurgery*, **116** (2012), 1172–1181.

[50] H. Schättler, U. Ledzewicz, Y. Kim, A. de los Reyes and E. Jung, On the control of cell migration and proliferation in glioblastoma in *52nd IEEE Conference on Decision and Control*, Florence, Italy, (2013), 1810–1815.

[51] G. S. Stamatakos, V. P. Antipas and N. K. Uzunoglu, A spatiotemporal, patient individualized simulation model of solid tumor response to chemotherapy in vivo: the paradigm of glioblastoma multiforme treated by temozolomide, *IEEE Transactions on Biomedical Engineering*, **53** (2006), 1467–1477.

[52] G. Stamatakos, V. Antipas, N. Uzunoglu and R. Dale, A four-dimensional computer simulation model of the in vivo response to radiotherapy of glioblastoma multiforme: studies on the effect of clonogenic cell density, *The British Journal of Radiology*, **79** (2004), 389–400.

[53] A. M. Stein, T. Demuth, D. Mobley, M. Berens and L. M. Sander, A mathematical model of glioblastoma tumor spheroid invasion in a three-dimensional *in vitro* experiment, *Biophysical Journal*, **92** (2007), 356–365.

[54] A. M. Stein, M. O. Nowicki, T. Demuth, M. E. Berens, S. E. Lawler, E. A. Chiocca and L. M. Sander, Estimating the cell density and invasive radius of three-dimensional glioblastoma tumor spheroids grown in vitro, *Applied Optics*, **46** (2007), 5110–5118.

[55] R. Stupp, W. P. Mason, M. J. Van Den Bent, M. Weller, B. Fisher, M. J. Taphoorn, K. Belanger, A. A. Brandes, C. Marosi and U. Bogdahn et al., Radiotherapy plus concomitant and adjuvant temozolomide for glioblastoma, *New England Journal of Medicine*, **352** (2005), 987–996.

[56] R. Sullivan and C. H. Graham, Hypoxia-driven selection of the metastatic phenotype, *Cancer and Metastasis Reviews*, **26** (2007), 319–331.

[57] K. Swanson, E. Alvord and J. Murray, A quantitative model for differential motility of gliomas in grey and white matter, *Cell Proliferation*, **33** (2000), 317–330.

[58] K. Swanson, H. Harpold, D. Peacock, R. Rockne, C. Pennington, L. Kilbride, R. Grant, J. Wardlaw and E. Alvord Jr, Velocity of radial expansion of contrast-enhancing gliomas and the effectiveness of radiotherapy in individual patients: A proof of principle, *Clinical Oncology*, **20** (2008), 301–308.

[59] K. R. Swanson, R. C. Rockne, J. Claridge, M. A. Chaplain, E. C. Alvord and A. R. Anderson, Quantifying the role of angiogenesis in malignant progression of gliomas: in silico modeling integrates imaging and histology, *Cancer Research*, **71** (2011), 7366–7375.

[60] M. D. Szeto, G. Chakraborty, J. Hadley, R. Rockne, M. Muzi, E. C. Alvord, K. A. Krohn, A. M. Spence and K. R. Swanson, Quantitative metrics of net proliferation and invasion link biological aggressiveness assessed by mri with hypoxia assessed by fmiso-pet in newly diagnosed glioblastomas, *Cancer Research*, **69** (2009), 4502–4509.

[61] J. P. Tian, A. Friedman, J. Wang and E. A. Chiocca, Modeling the effects of resection, radiation and chemotherapy in glioblastoma, *Journal of Neuro-oncology*, **91** (2009), 287–293.

[62] P. Tracqui, G. Cruywagen, D. Woodward, G. Bartoo, J. Murray and E. Alvord, A mathematical model of glioma growth: The effect of chemotherapy on spatio-temporal growth, *Cell Proliferation*, **28** (1995), 17–31.

[63] S. Turner and J. A. Sherratt, Intercellular adhesion and cancer invasion: A discrete simulation using the extended potts model, *Journal of Theoretical Biology*, **216** (2002), 85–100.

[64] A. Valster, N. L. Tran, M. Nakada, M. E. Berens, A. Y. Chan and M. Symons, Cell migration and invasion assays, *Methods*, **37** (2005), 208–215.

[65] C. H. Wang, J. K. Rockhill, M. Mrugala, D. L. Peacock, A. Lai, K. Jusenius, J. M. Wardlaw, T. Cloughesy, A. M. Spence and R. Rockne et al., Prognostic significance of growth kinetics in newly diagnosed glioblastomas revealed by combining serial imaging with a novel biomathematical model, *Cancer Research*, **69** (2009), 9133–9140.

[66] S. M. Wise, J. S. Lowengrub, H. B. Frieboes and V. Cristini, Three-dimensional multispecies nonlinear tumor growth—i: Model and numerical method, *Journal of Theoretical Biology*, **253** (2008), 524–543.

[67] D. Yang, J. P. Tian and J. Wang, A solvable hyperbolic free boundary problem modelling tumour regrowth, *Applicable Analysis*, **92** (2013), 1541–1558.

[68] E. I. Zacharaki, C. S. Hogea, G. Biros and C. Davatzikos, A comparative study of biomechanical simulators in deformable registration of brain tumor images, *IEEE Transactions on Biomedical Engineering*, **55** (2008), 1233–1236.

[69] X. Zheng, S. Wise and V. Cristini, Nonlinear simulation of tumor necrosis, neo-vascularization and tissue invasion via an adaptive finite-element/level-set method, *Bulletin of Mathematical Biology*, **67** (2005), 211–259.

Received May 30, 2014; Accepted December 09, 2014.

E-mail address: nmartirosyan@email.arizona.edu
E-mail address: Erica.Rutter@asu.edu
E-mail address: WyattRamey@creighton.edu
E-mail address: kostelich@asu.edu
E-mail address: kuang@asu.edu
E-mail address: Mark.Preul@dignityhealth.org